Electronic Supplementary Material

Carbon vacancy-assisted stabilization of individual Cu_5 clusters on graphene. Insights from *ab initio* molecular dynamics

Lenard Carroll,[a] Lyudmila V. Moskaleva,[a*] and María Pilar de Lara-Castells[b*]

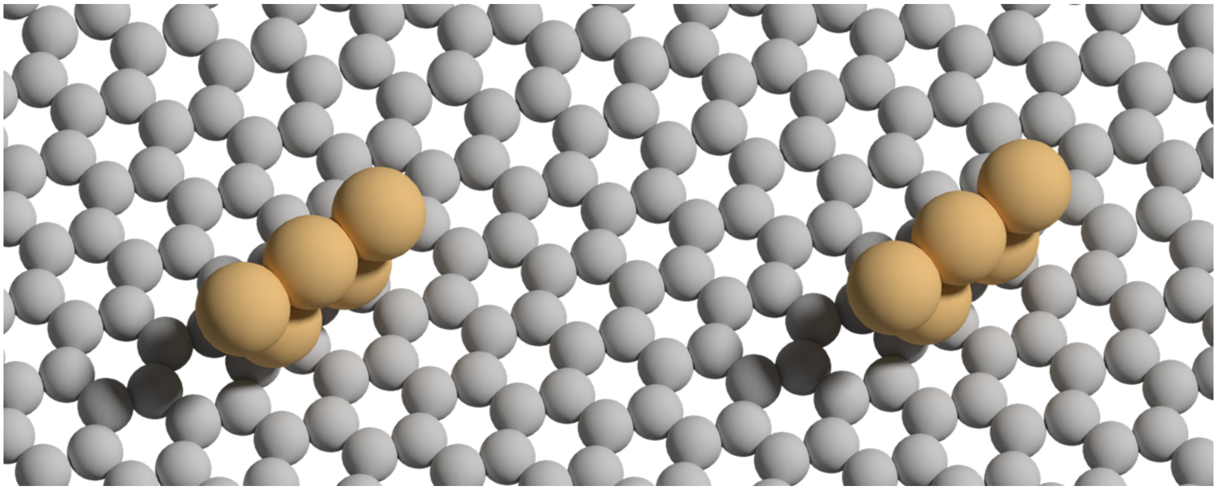

1 Constrained graphene AIMD simulations

We present here *ab initio* molecular dynamics (AIMD) simulation results for the adsorption of two planar Cu_5 clusters on a constrained (fixed) graphene sheet, both pristine and defective. In the case of the defective sheet, the clusters were placed near the vacancies resulting in an optimized structure where the Cu_5 clusters "fell" into the vacancy. This section provides snapshots of the simulations and shows the minimum distances between the Cu atoms and between C and Cu atoms on the graphene support. We also illustrate the time-dependent evolution of the root mean square deviation (RMSD) of the individual Cu atoms on the support system.

1.1 Interaction of two Cu_5 clusters on a defect-free graphene sheet. Dimerization

This AIMD simulation highlights the dimerization process of two 2D-Cu_5 clusters into a highly stable Cu_{10} dimer formed by two anchored 3D-Cu_5 structures. The process can be divided into three steps, namely, cluster diffusion, Cu_5–Cu_5 attraction and aggregation into a structure made of two planar fragments, and geometrical transformation into the final structure composed of two anchored 3D-Cu_5 bipyramidal arrangements. These steps are reflected in the time-evolution of the RMSDs of the copper atomic positions, with the Cu

---

[a] *Department of Chemistry, University of the Free State, PO Box 339, Bloemfontein 9300, South Africa. E-mail: lyudmila.moskaleva@gmail.com*

[b] *Institute of Fundamental Physics (AbinitSim Unit), Consejo Superior de Investigaciones Científicas (CSIC), E-28006 Madrid, Spain. E-mail: Pilar.deLara.Castells@csic.es*

atoms undergoing wide and uneven amplitude motions, acquiring different RMSDs during steps 2 and 3.

The onset of step 3 can also be distinguished in the evolution of the minimum inter-cluster Cu–Cu distance, which features an abrupt drop to an almost constant value at around 40 ps, indicating the existence of at least one Cu–Cu bond between the two Cu_5 fragments from this point onward. The interaction between the two Cu_5 clusters in this configuration is 1.4 eV less attractive at the DFT-D3 level than in the structure composed of anchored 3D–Cu_5 clusters, explaining why the structure evolves towards the latter more energetically stable complex from 44 to 62 ps.

1.2 Interaction of two Cu_5 clusters on a graphene sheet with double carbon vacancies. Confinement

In this scenario, two Cu_5 clusters interact on a graphene sheet with double carbon vacancies. During the geometry optimization, the 2D-Cu_5 clusters became trapped by the carbon vacancies and underwent a frustrated rotational motion, eventually transforming into anchored 3D-Cu_5 geometrical arrangements. The binding of the 3D-Cu_5 clusters to the cavity of the support was stronger than for the 2D–Cu_5 counterparts, but the minimum Cu–C distances increased slightly. However, the minimum intra-cluster distances remained largely unaffected by the geometrical transformation. The 3D–Cu_5 clusters rotated around the cavity, exhibiting stable behavior during the rest of the simulation. The non-anchored Cu atoms of the clusters underwent a collective rotational motion around the axis passing through the immobilized Cu atom in the last approximately 30 ps of the simulation. The electronic structures of the Cu_5 clusters were preserved upon anchoring onto the vacancy site, indicating that the vacancy did not perturb the electronic structure of the supported Cu_5 cluster to a larger extent than in the defect-free carbon-based sheet. The interaction between Cu_5/graphene was found to be dispersion-dominated, indicating that the Cu_5 cluster was not significantly perturbed by the support.

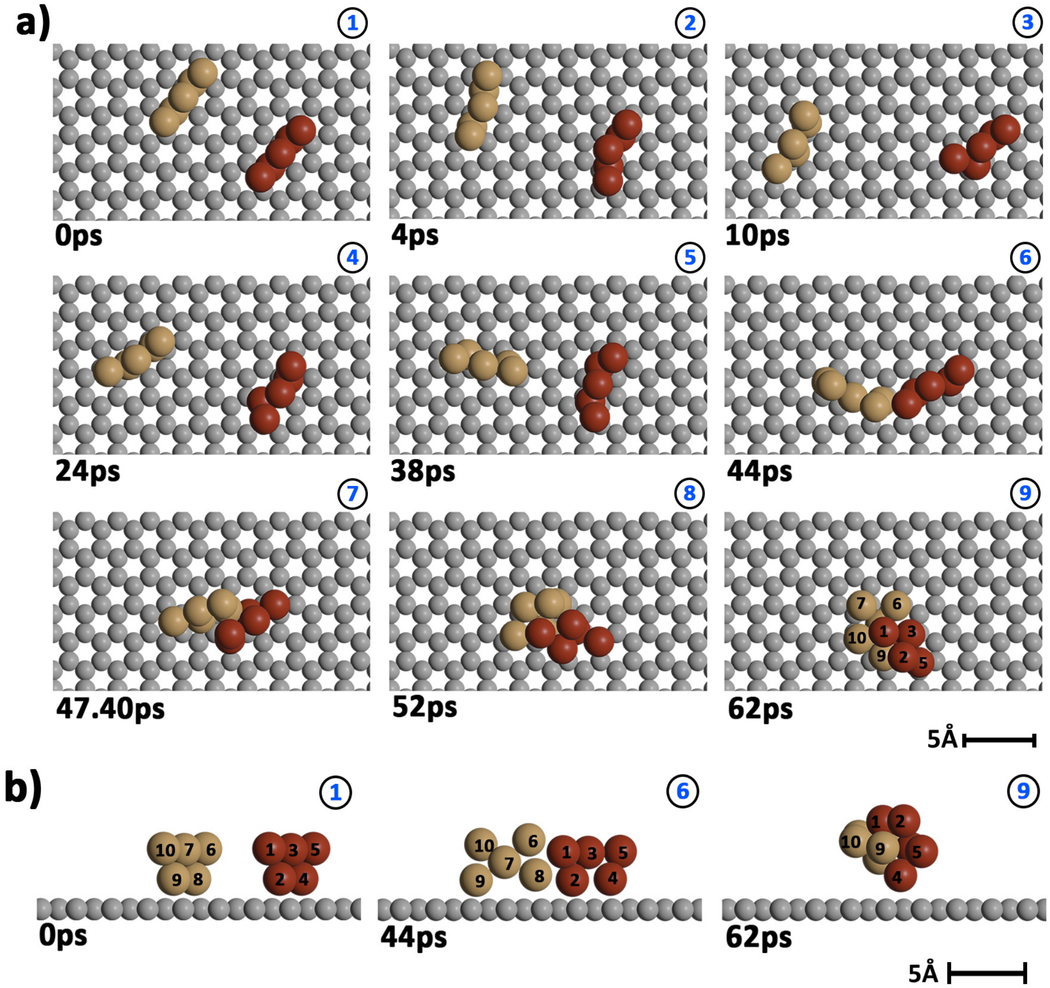

Figure S1: Snapshots showing the evolution of two Cu_5 clusters (Cu atoms of the two clusters shown in brown and red) previously deposited onto a defect-free graphene surface (C atoms in gray) at a temperature of 400 K. a) Top view; b) Side view.

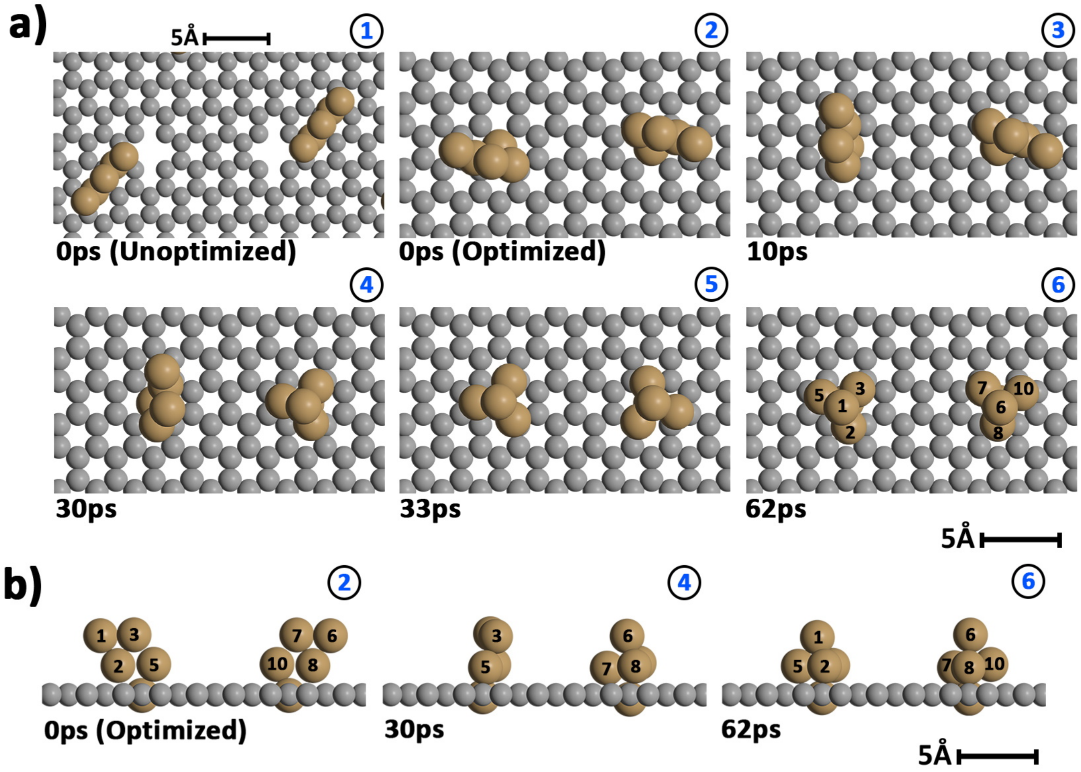

Figure S2: Snapshots showing the evolution of two Cu_5 clusters (Cu atoms in brown) previously deposited onto a graphene sheet containing two carbon vacancies (C atoms in gray) at a temperature of 400 K. a) Top view; b) Side view.

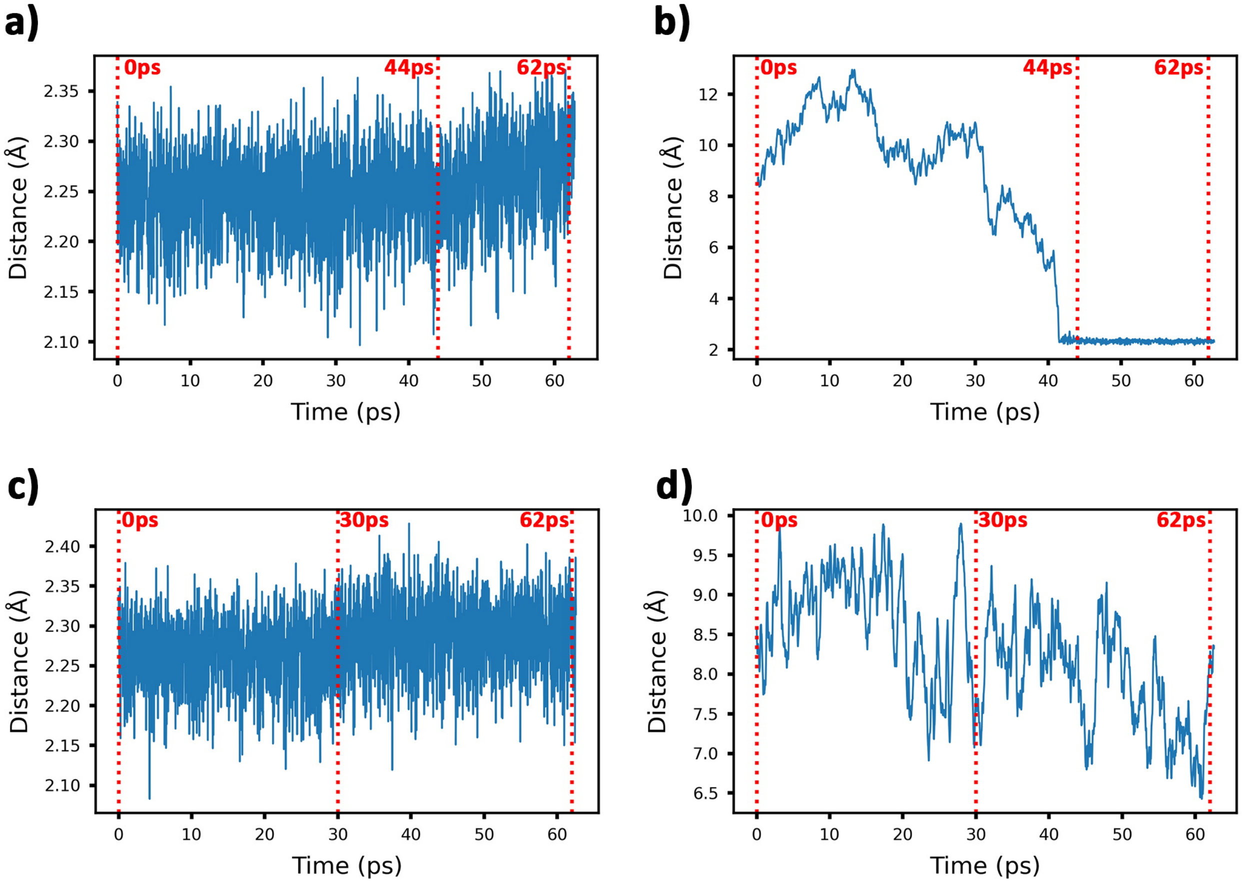

Figure S3: Panel a) Evolution of the minimum intra-cluster Cu–Cu distance. Defect-free graphene; Panel b) Evolution of the minimum inter-cluster Cu–Cu distance. Defect-free graphene surface; Panel c) Evolution of the minimum intra-cluster Cu–Cu distance on defected graphene; Panel d) Evolution of the minimum inter-cluster Cu–Cu distances on defected graphene.

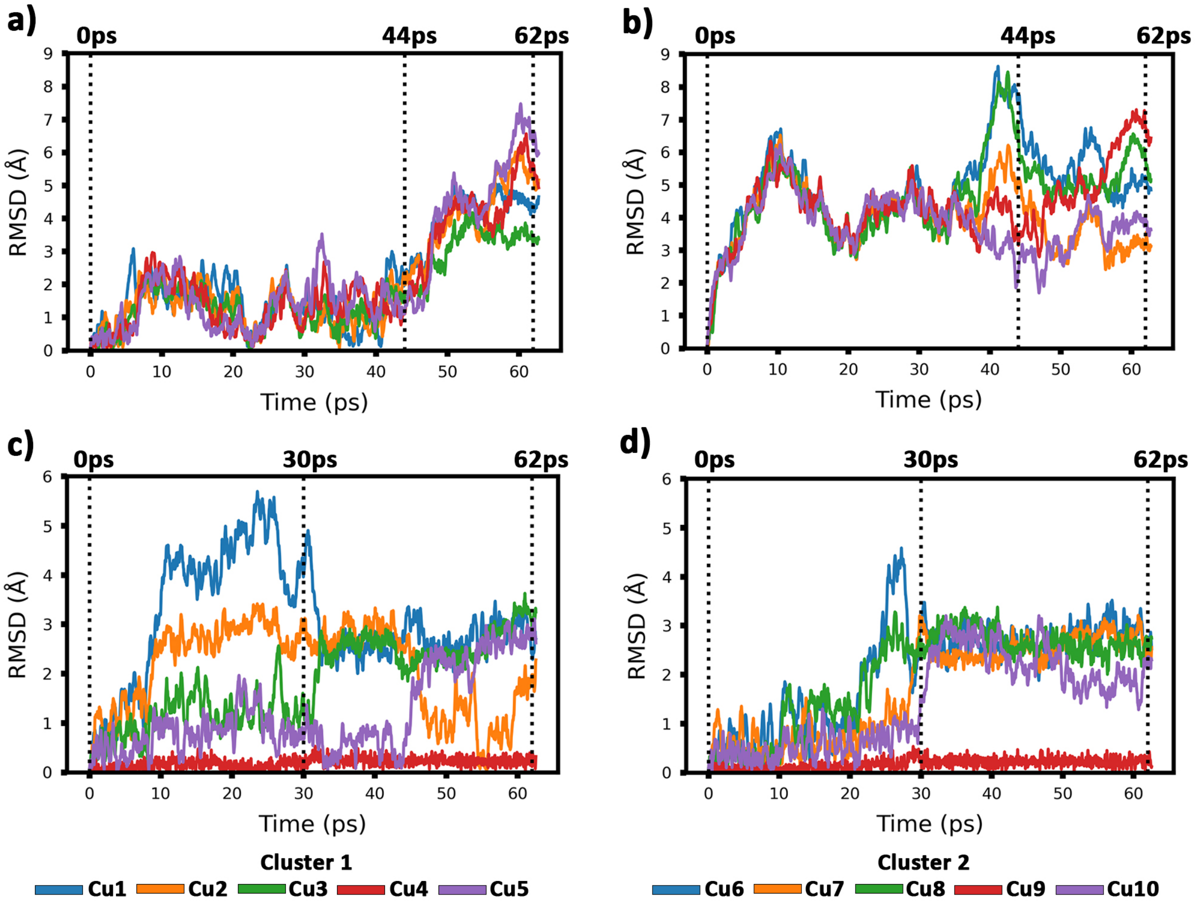

Figure S4: Root-mean-square deviations (RMSDs) of copper atomic positions for the two Cu_5 clusters supported on defect-free graphene [panels a) and b)] and supported on defected graphene [panels c) and d)] (see also Figures S2 and S3).

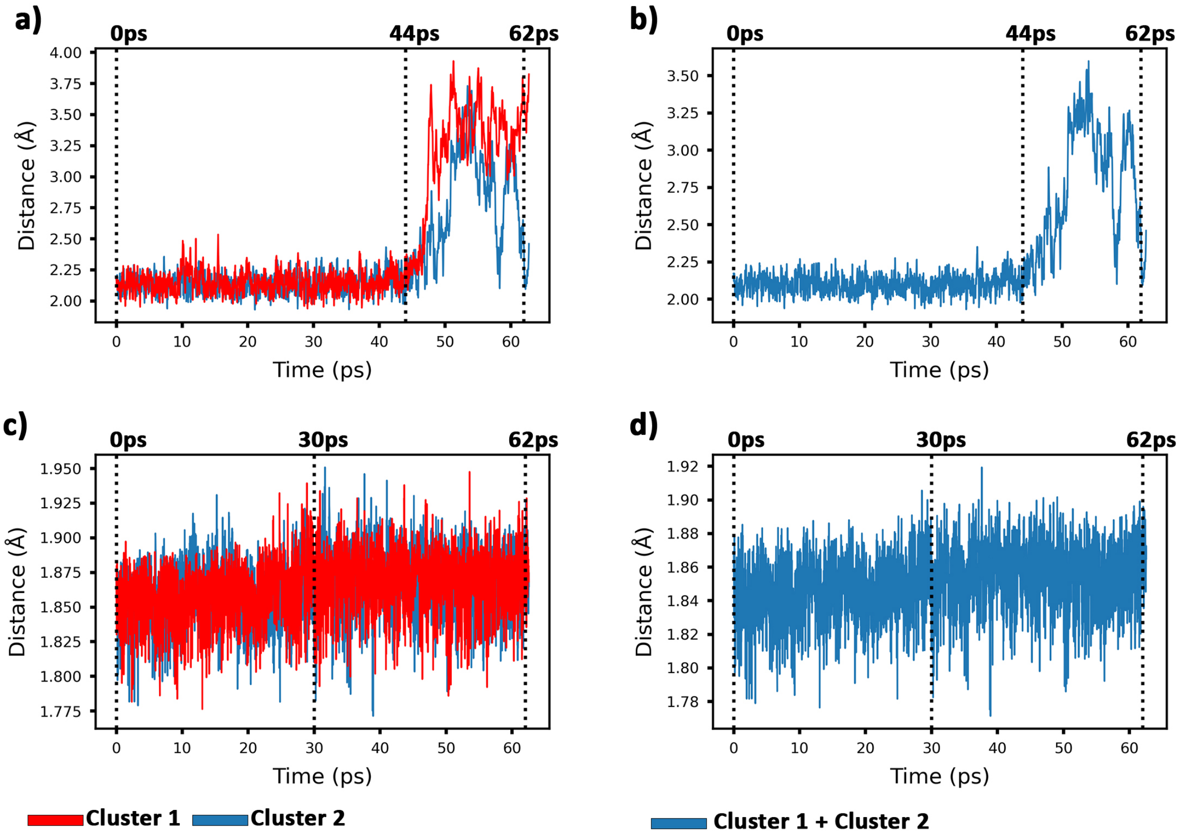

Figure S5: Time-dependent evolution of the minimum C–Cu distances for a) the interaction of the two 2D-Cu_5 clusters with defect-free graphene; b) the interaction of all Cu atoms with defect-free graphene; c) the interaction of the two 2D–Cu_5 clusters with defected graphene; d) the interaction of all Cu atoms with defected graphene.

2 Unconstrained graphene AIMD simulation (600 K)

We present here an AIMD simulation of two Cu_5 clusters on unconstrained (relaxed) pristine graphene at 600 K. This simulation was conducted for 42 ps and resulted in a faster simulation time of 34 ps before the dimerization process started. The simulation revealed that one of the Cu_5 clusters underwent a transformation from planar to three-dimensional around 18 ps into the simulation. After this transformation, the two clusters did not move closer to each other until just after 30 ps, where they rapidly dimerized.

Cluster 1 experienced only small movements within the first 18 ps and became more mobile after cluster 2's transformation, while cluster 2 underwent rapid changes within the first 10 ps of the simulation. The distance between the Cu_5 clusters initially increased up to around 8 ps, but after cluster 2's transformation, the distance gradually increased until just before the start of the dimerization process. Once dimerization began, there was a sharp decrease in distance. The minimum distance between C and Cu atoms only increased up to 3.4 Å (for cluster 2) as compared to 4.5 Å for the 400 K run.

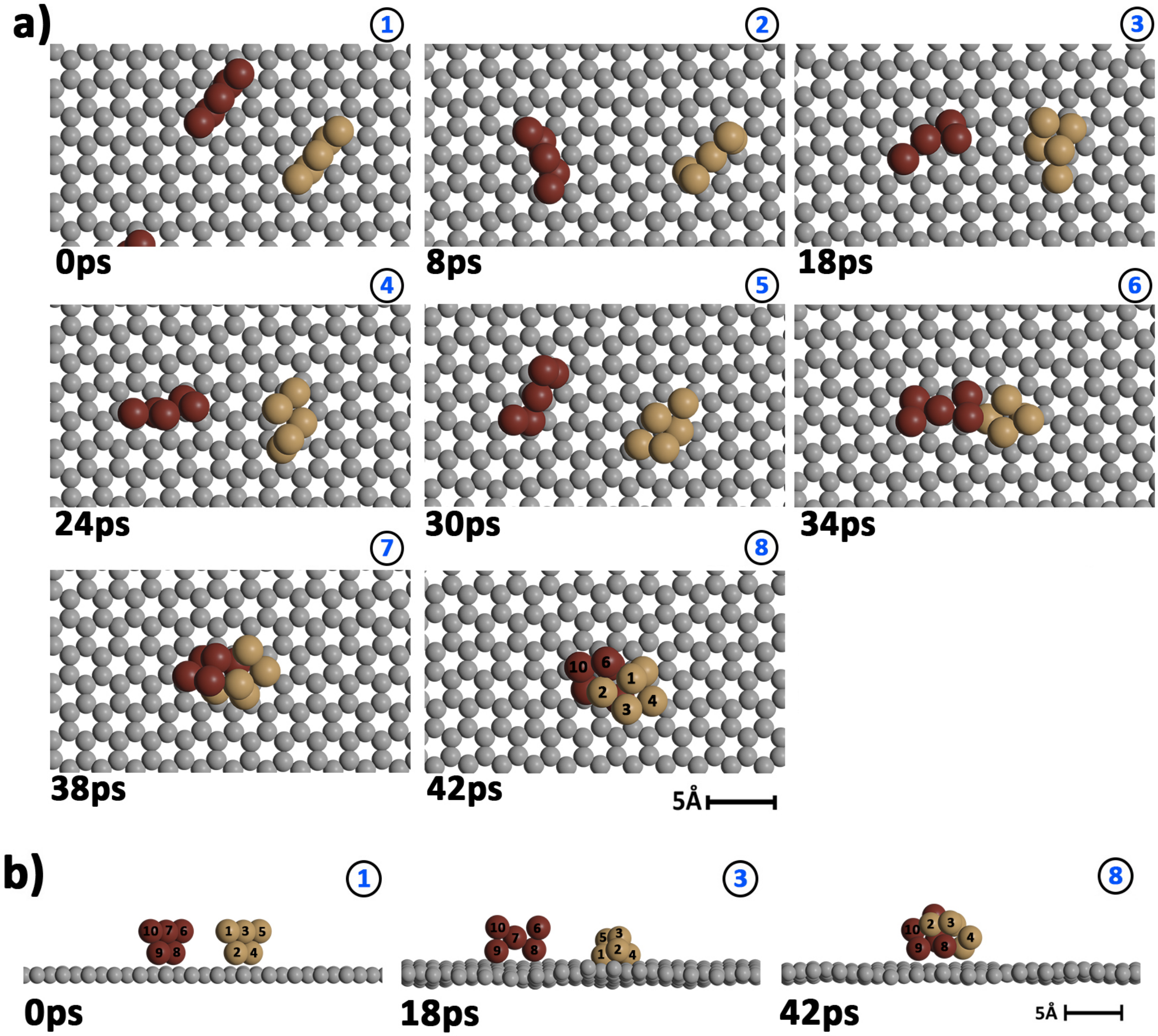

Figure S6: Snapshots showing the evolution of two Cu_5 clusters (Cu atoms in brown) previously deposited onto a relaxed defect-free graphene sheet (C atoms in gray) at a temperature of 600 K. a) Top view; b) Side view.

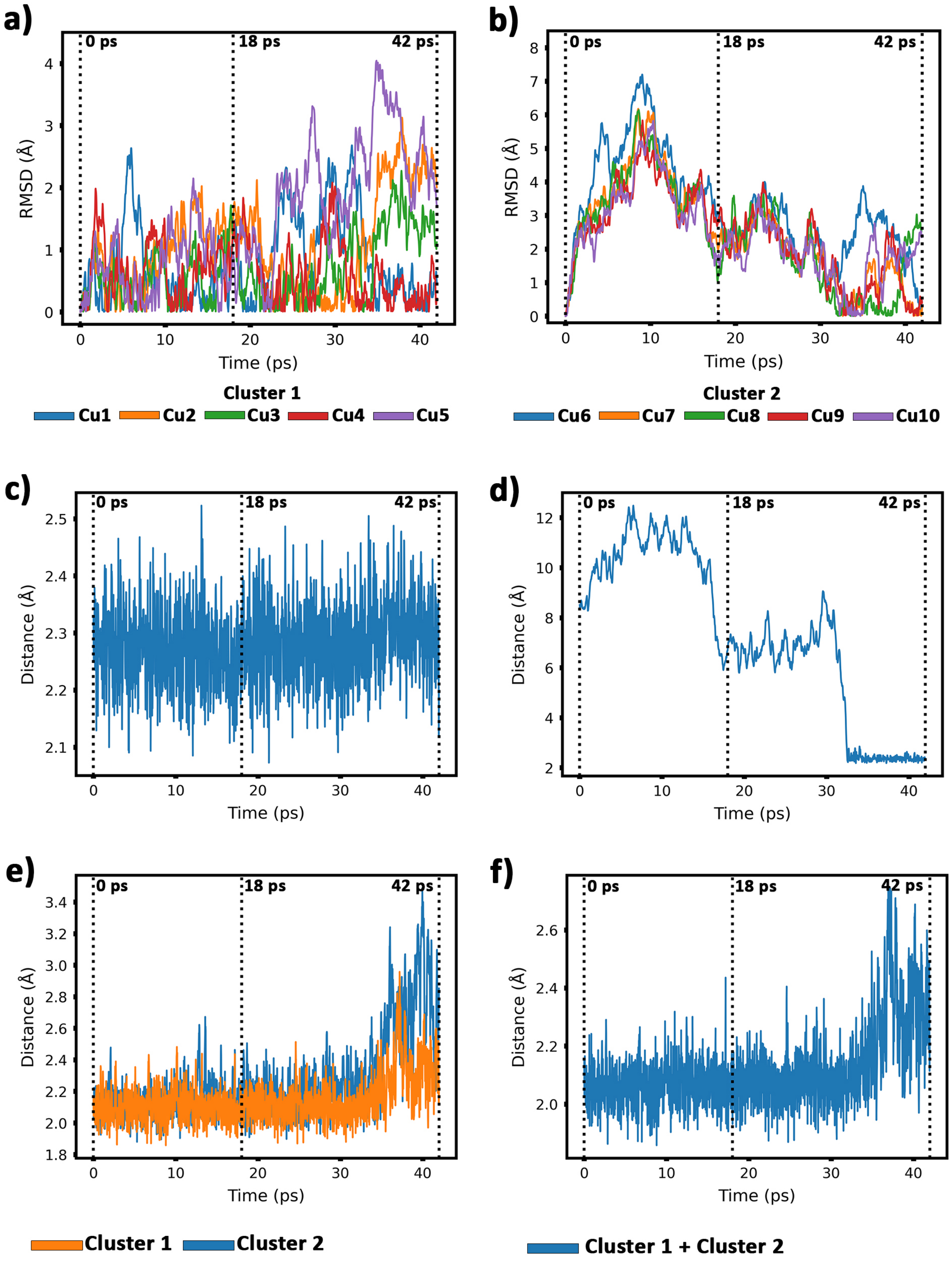

Figure S7: Root-mean-square deviations (RMSDs) of copper atomic positions for the two Cu_5 clusters supported on relaxed defect-free graphene at 600 K [panels a) and b)]; Panel c) Evolution of the minimum intra-cluster Cu–Cu distance. Defect-free graphene; Panel d) Evolution of the minimum inter-cluster Cu–Cu distance. Defect-free graphene surface; Time-dependent evolution of the minimum C–Cu distances for e) the interaction of the two 2D-Cu_5 clusters with defect-free graphene; f) the interaction of all Cu atoms with defect-free graphene.

3 Unconstrained graphene AIMD simulation (300 K)

We present here an AIMD simulation of two Cu_5 clusters on relaxed pristine graphene at 300 K. This simulation was conducted for 62 ps and resulted in a faster simulation time (compared to 400 K, but not 600 K) of 35 ps before the dimerization process started. Unlike the 600 K simulation, but similar to the 400 K run, the Cu_5 clusters do not undergo any geometrical transformations here, and with less thermal energy available at 300 K to explore different configurations and motions, less rotation of the clusters are observed as compared to the 400 K run. From the RMSD plots in Figure S9a-b, for the most part of the simulation up to before the dimerization process starts, the Cu atoms in both clusters move as a collective unit, with the RMSD values being very similar for each Cu atom per cluster. Cluster 2, however, is more mobile before the dimerization as is the same for all the other runs too. In Figure S9d, we observe that the Cu clusters shortly move apart on the graphene support, but unlike the 400 and 600 K run, this is a more shortened time until we observe the clusters moving closer to each other. There is also a less rapid decrease between the minimum distance for the inter-cluster Cu atoms, unlike for the other temperatures, that being said, there is still a sharp decrease in this distance beyond 30 to 35 ps. Furthermore, according to Figures S9e-f, there is also a less significant change in the minimum C–Cu distance as compared to the 400 K run.

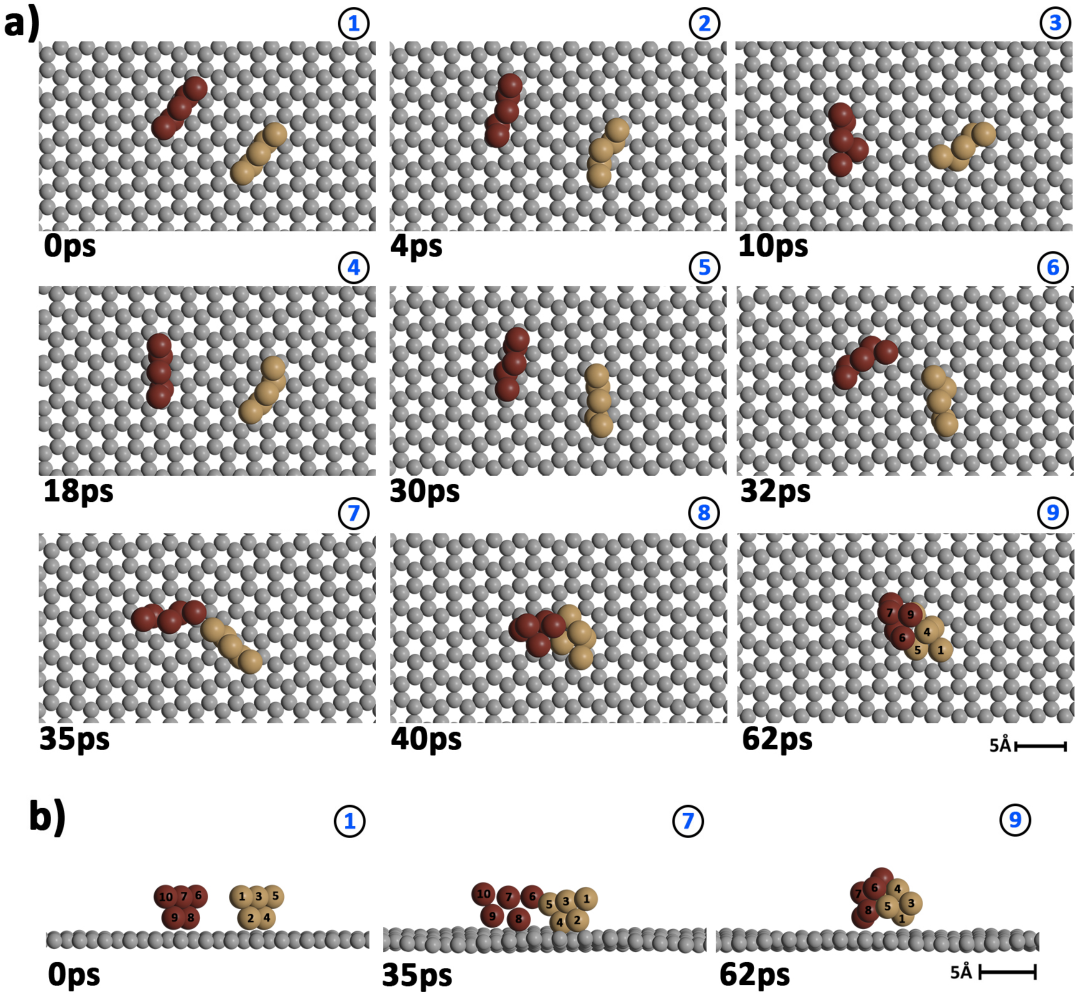

Figure S8: Snapshots showing the evolution of two Cu_5 clusters (Cu atoms in brown) previously deposited onto a relaxed defect-free graphene sheet (C atoms in gray) at a temperature of 300 K. a) Top view; b) Side view.

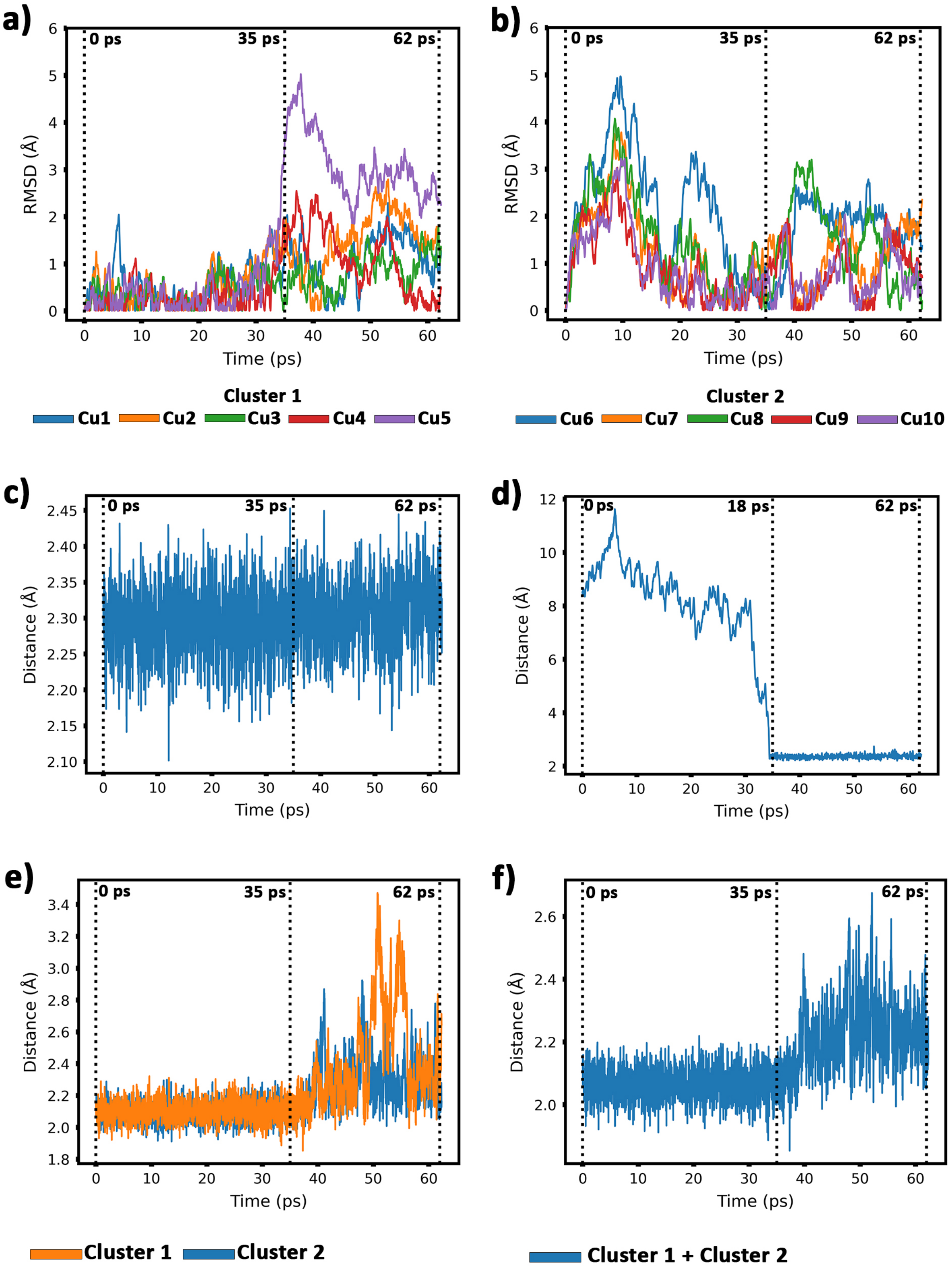

Figure S9: Root-mean-square deviations (RMSDs) of copper atomic positions for the two Cu_5 clusters supported on relaxed defect-free graphene at 300 K [panels a) and b)]; Panel c) Evolution of the minimum intra-cluster Cu–Cu distance. Defect-free graphene; Panel d) Evolution of the minimum inter-cluster Cu–Cu distance. Defect-free graphene surface; Time-dependent evolution of the minimum C–Cu distances for e) the interaction of the two 2D–Cu_5 clusters with defect-free graphene; f) the interaction of all Cu atoms with defect-free graphene.

4 Comparison between CP2K and VASP

The results obtained with the VASP and CP2K code are in excellent agreement with each other. To illustrate this, we calculated the adsorption energies for planar and trigonal bipyramidal Cu_5 clusters on pristine and defective graphene surfaces (only sampling the Gamma point), using both VASP and CP2K for comparison. The results, presented in Table S1 and Table S2 below, show a small absolute percentage difference of 0.32% – 5.1% between the adsorption energies calculated using the two codes, indicating a high level of agreement between them. We also calculated the gas-phase interaction energy for Cu_{10} in VASP and CP2K, with the former having a value of −5.41 eV and the latter −5.40 eV, an excellent agreement. On graphene, the interaction energies are −4.20 eV for CP2K and −4.17 eV for VASP. 5×5×1 k-points were applied for both, and D3 dispersion corrections employed.

Table S1: Adsorption energies (in eV) of two planar Cu_5 clusters on a (6×10) graphene supercell. Gamma point only sampling was used.

CP2K				
Type	**Fixed No Dispersion**	**Fixed w/ Dispersion**	**Relaxed No Dispersion**	**Relaxed w/ Dispersion**
Pristine	−1.05	−2.58	−1.43	−2.57
Defective	−1.65	−3.16	−2.25	−3.53
VASP				
Pristine	−1.00	−2.55	−1.41	−2.55
Defective	−1.57	−3.17	−2.22	−3.50

Table S2: Adsorption energies (in eV) of one 2D or 3D Cu_5 cluster on a (6×10) pristine graphene supercell. Gamma point only sampling was used.

2D		
Code	**Fixed w/ Dispersion**	**Relaxed w/ Dispersion**
CP2K	−1.17	−1.25
VASP	−1.14	−1.24
3D		
CP2K	−0.94	−1.04
VASP	−0.93	−1.03

5 Comparison between single gamma point and 5×5×1 k-points mesh

A table below shows a comparison of adsorption energies of two planar Cu_5 clusters calculated with gamma point only sampling and a 5×5×1 k-point mesh. In some cases there is a notable deviation of up to 0.3 eV but the trends are not altered. We believe this difference in energy is most likely due to a small difference in the structures. We used the Gamma point only approach for the AIMD simulation, as this is the only affordable option; however, all energies reported in the manuscript have been calculated using a 5×5×1 k-point mesh.

Furthermore, we compared the interaction energy of two Cu_5 clusters in a Cu_{10} dimer on a relaxed pristine graphene support (with dispersion corrections applied) using either the Gamma point only sampling or a 5×5×1 k-point mesh, with the former approach yielding

−4.26 eV and the latter, −4.20 eV, a difference of only 1.43%. When considering the interaction energy in the gas-phase, using Gamma point only sampling yields a value of −5.4013 eV, while using a 5×5×1 k-point mesh yields a value of −5.4012 eV, a difference of less than 0.2%.

Table S3: Adsorption energies (in eV) of two co-adsorbed planar Cu_5 clusters on a (6x10) graphene supercell using Gamma point only and 5×5×1 k-points sampling.

Type	**Fixed No Dispersion [Gamma point only]**	**Fixed No Dispersion [5×5×1 k points]**	**Relaxed w/ Dispersion [Gamma point only]**	**Relaxed w/ Dispersion [5×5×1 k points]**
Pristine	−1.05	−1.07	−2.57	−2.54
Defective	−1.65	−1.36	−3.53	−3.47

We confirmed these values with VASP, which are in good agreement with the CP2K values, including an almost 0.3 eV difference for fixed defective graphene (no dipsersion) going from single gamma point to 5×5×1 k-points.

Table S4: Adsorption energies (in eV) of two co-adsorbed planar Cu_5 clusters on a (6x10) graphene supercell using 5×5×1 k-points sampling, VASP & CP2K.

Type	**Fixed No Dispersion [5×5×1 k points] CP2K**	**Fixed No Dispersion [5×5×1 k points] VASP**	**Relaxed w/ Dispersion [5×5×1 k points] CP2K**	**Relaxed w/ Dispersion [5×5×1 k points] VASP**
Pristine	−1.07	−1.02	−2.54	−2.51
Defective	−1.36	−1.26	−3.47	−3.41

6 Structure Comparison

Below are figures showing the structures of some of the most stable Cu_5 isomers on graphene, with their adsorption energies also included. All these calculations were done using a 5×5×1 k-point mesh with D3 dispersion corrections applied.

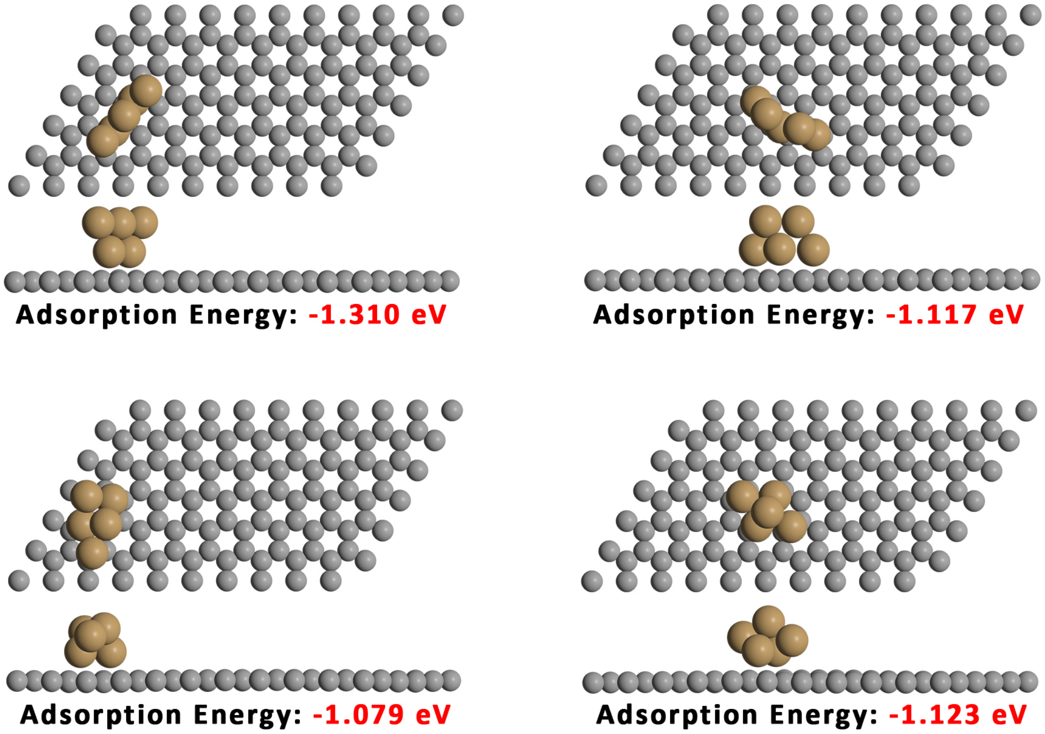

Figure S10: Adsorption energies of various single 2D and 3D Cu_5 clusters adsorbed on a (6×10) graphene supercell, calculated at the PBE-D3 level using 5×5×1 Monkhorst-Pack k-point mesh for sampling the Brillouin zone. The adsorption energies were calculated relative to the lowest-energy gas-phase isomer (2D–Cu_5).

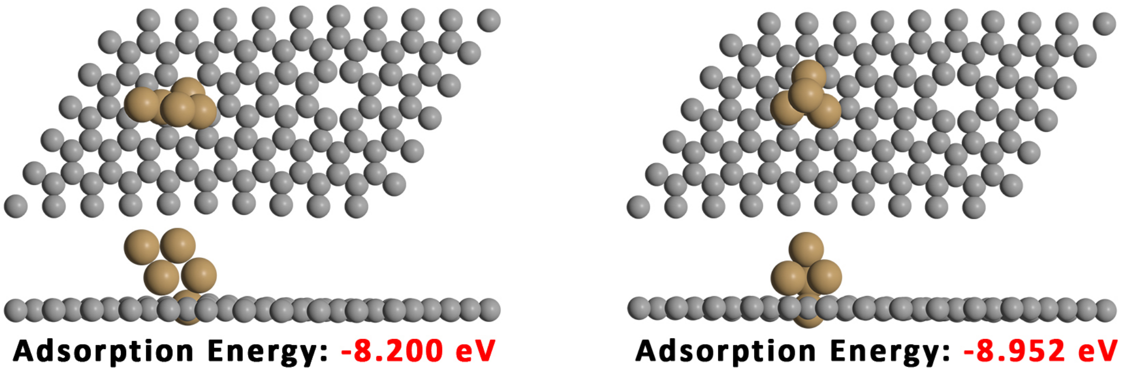

Figure S11: Adsorption energies of a planar and trigonal bipyramidal Cu_5 cluster adsorbed into a (6×10) graphene supercell vacancy, calculated at the PBE-D3 level using 5×5×1 Monkhorst-Pack k-point mesh for sampling the Brillouin zone. The adsorption energies were calculated relative to the lowest-energy gas-phase isomer (2D–Cu_5).

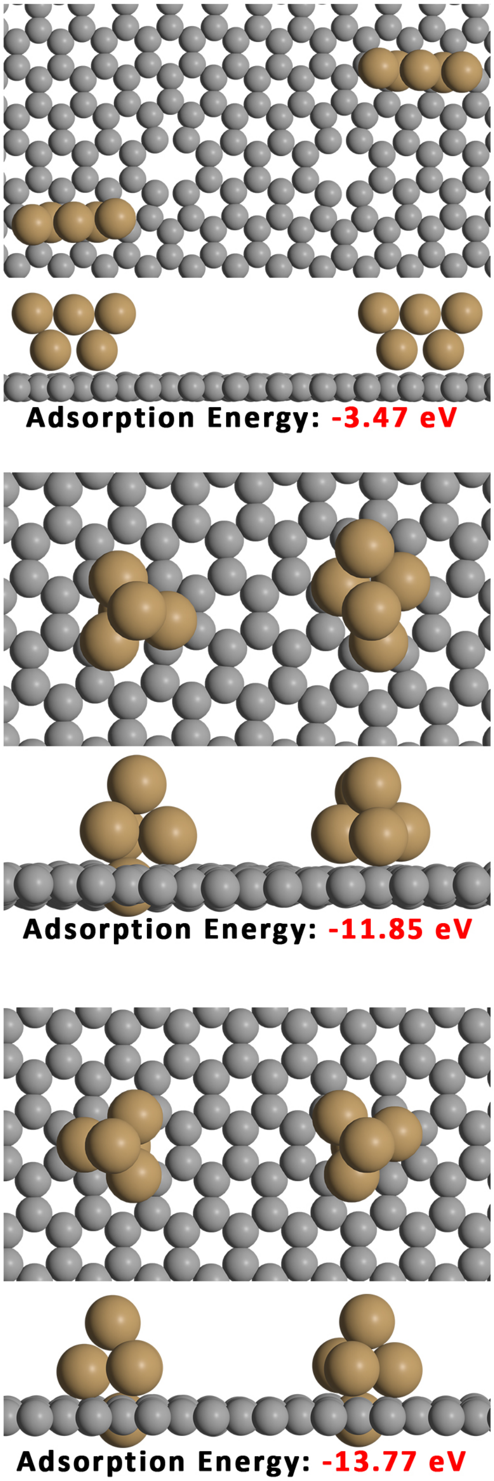

Figure S12: Adsorption energies of a planar and trigonal bipyramidal Cu_5 clusters adsorbed on or into (6×10) graphene supercell vacancies, calculated at the PBE-D3 level using 5×5×1 Monkhorst-Pack k-point mesh for sampling the Brillouin zone. The adsorption energies were calculated relative to the lowest-energy gas-phase isomer (2D–Cu_5).

7 Cohesive Energies for Cu_5 and Cu_{10} using CP2K

The CP2K cohesive energies were calculated with and without D3-Dispersion correction and the 5×5×1 k-points mesh approach as follows:

Cu_5 (Planar; Dispersion) = −8.98 eV or −1.80 eV/atom
Cu_5 (Trigonal Bipyramidal; Dispersion) = −8.75 eV or −1.75 eV/atom
Cu_{10} (Dispersion) = −23.37 eV or −2.34 eV/atom
Cu_5 (Planar; No Dispersion) = −8.74 eV or −1.75 eV/atom
Cu_5 (Trigonal Bipyramidal; No Dispersion) = −8.40 eV or −1.68 eV/atom
Cu_{10} (No Dispersion) = −22.36 eV or −2.24 eV/atom

These values are in good agreement with what has been reported in literature both theoretically [1], and experimentally.[2] For the former, the Cu_5 and Cu_{10} values are approximately −1.74 eV/atom and −2.2 eV/atom. For the latter the cohesive energies can be calculated for the Cu_5 cluster by summing the dissociation energies (presented in the paper) and dividing it by the nuclearity, resulting in a value of -1.55 ± 0.15 eV/atom.

References

[1] U. Rangel-Peña, R. Camacho-Mendoza, S. González-Montiel, L. Feria and J. Cruz-Borbolla, *J. Clust. Sci.*, 2021, **32**, 1155—-1173.

[2] V. Spasov, T.-H. Lee and K. M. Ervin, *J. Chem. Phys.*, 2000, **112**, 1713–1720.